

# Adsorption and Photocatalytic Decomposition of Amino Acids in TiO<sub>2</sub> Photocatalytic Systems<sup>†</sup>

Trung H. Tran, Atsuko Y. Nosaka,\* and Yoshio Nosaka\*

Department of Chemistry, Nagaoka University of Technology, Kamitomioka, Nagaoka 940-2188, Japan

Received: August 15, 2006; In Final Form: September 21, 2006

The adsorption and photodecomposition of seven kinds of amino acids on a TiO<sub>2</sub> surface were investigated by zeta potential measurements and <sup>1</sup>H NMR spectroscopy in TiO<sub>2</sub> aqueous suspension systems. The decomposition rates increased in the order of Phe < Ala < Asp < Trp < Asn < His < Ser. For Phe, Trp, Asn, His, and Ser, the isoelectric point (IEP) of TiO<sub>2</sub> shifted to a lower pH with increasing decomposition rates upon adsorption on TiO<sub>2</sub>, suggesting that the effective adsorption and photocatalytic sites for these amino acids should be the basic terminal OH on the solid surface. Since the amino acids that decomposed faster than the others contain –OH (Ser), –NH (Trp, His), or –NH<sub>2</sub> (Asn) in their side chain, they are considered to interact with the basic terminal OH groups more preferably by the side chain and are vulnerable to photocatalytic oxidation. On the other hand, Ala interacts with the acidic bridged OH on TiO<sub>2</sub> to cause an IEP shift to a higher pH. The correlation of the surface hydroxyl groups with the photocatalysis of amino acids was verified by the use of calcined TiO<sub>2</sub> without surface hydroxyl groups.

## Introduction

Among the various semiconductor materials, titanium dioxide is one of the most widely studied metal oxides.<sup>1–8</sup> The irradiation of TiO<sub>2</sub> by UV light with a photon energy higher than its band gap generates excited-state electrons and holes at the conduction band and the valence band, respectively. These electrons and holes can initiate various redox reactions at the metal oxide surface. In the presence of O<sub>2</sub> and H<sub>2</sub>O, the electrons and holes generate various active oxygen species. Organic molecules incorporated into the TiO<sub>2</sub> photocatalytic systems are decomposed through direct oxidization by the photogenerated holes. Thus, TiO<sub>2</sub> has the potential to oxidize a wide range of environmentally hazardous organic contaminants into harmless compounds such as CO<sub>2</sub> and H<sub>2</sub>O. Hence, the TiO<sub>2</sub> photocatalyzed oxidation process has been widely investigated in the context of the purification of waters contaminated by organic chemicals.<sup>7,8</sup> Besides high oxidation power, TiO<sub>2</sub> has prominent properties such as chemical inertness, a photoinduced highly hydrophilic surface, and nontoxicity. Therefore, it has been widely applied to environmental cleanup, solar cells, antifogging, and self-cleaning mirrors and glasses.<sup>1–6</sup>

On the other hand, the application of TiO<sub>2</sub> in biological fields, such as antibacterial effects<sup>9–11</sup> and medical treatments for diseases, including cancer,<sup>12</sup> has also been extensively progressive. However, the mechanism underlying the photobiological activity of TiO<sub>2</sub> is not yet well understood. Saito et al. have shown that the bactericidal activity photocatalyzed by TiO<sub>2</sub> is accompanied by cell membrane damage observed as a loss of potassium ions, proteins, and RNA from bacterial cells.<sup>13</sup> The decomposition of proteins upon TiO<sub>2</sub> photocatalysis was reported by Muszkat et al. for serum albumin, ovalbumin, and gamma globulins.<sup>14,15</sup> They analyzed the amount of amino acids in decomposed proteins and the released amino acids.

One of the important factors affecting photocatalysis is the adsorption of reactant molecules on the TiO<sub>2</sub> surface. Since the photocatalytic process is expected to occur at the interface between the TiO<sub>2</sub> semiconductor and the liquid medium, the knowledge about the features of the adsorbed molecules is invaluable for the elucidation of the photocatalytic mechanism. In addition, the interface between protein molecules and inorganic materials has recently received much attention. Recent progress in combinatorial biology has made it possible to acquire amino acid sequences possessing specific affinities to their target inorganic materials (denoted as aptamers).<sup>16,17</sup> These aptamers have the potential to provide new approaches to construct novel interfaces of biomolecules and inorganic materials. Recently, Sano et al. studied the binding mechanism between a Ti-binding peptide and Ti surfaces suspected to be covered with a TiO<sub>2</sub> film. They identified the essential amino acid residues for the specific binding by monitoring the effect of the substitution of each residue in the amino acid sequence with an alanine residue on the specific binding and proposed a binding model.<sup>17</sup>

Proteins and peptides are composed of various kinds of amino acids. For the proper understanding of the adsorptive and photocatalytic interactions between the TiO<sub>2</sub> surface and proteins/peptides, fundamental knowledge on the adsorption and photocatalytic reactivity of individual constituent amino acids would be essential. Hidaka and co-workers investigated the photomineralization of a series of amino acids upon TiO<sub>2</sub> photocatalysis by measuring the CO<sub>2</sub> evolution and the conversion of the amine group to NH<sub>4</sub><sup>+</sup> and NO<sub>3</sub><sup>–</sup> ions.<sup>18–20</sup> Amino acids are compounds that include –COOH and –NH<sub>2</sub> functional groups with various side chains on the α-carbon. The adsorption and decomposition are therefore expected to depend on the molecular structures of the amino acids.

<sup>1</sup>H NMR spectroscopy is one of the most effective techniques to investigate the change of molecular structures. One can observe directly the adsorption and decomposition of the reactant molecules by measuring the change of the signal intensities along with the formation of the decomposition intermediates,

<sup>†</sup> Part of the special issue “Arthur J. Nozik Festschrift”.

\* To whom correspondence should be addressed. Telephone: +81-258-47-9315. Fax: +81-258-47-9315. E-mail: nosaka@nagaokaut.ac.jp.

**TABLE 1: Amino Acids Examined and Figure Symbols Used in the in the Present Study**

Type of side chain	Amino acid	Abbreviated name	Structured of side chain R in $\text{H}_2\text{NCHRCOOH}$	Symbol
Aliphatic	Alanine	Ala	$-\text{CH}_3$	●
Aromatic	Phenyl alanine	Phe	$-\text{CH}_2-\text{C}_6\text{H}_5$	○
	Tryptophan	Trp	$-\text{CH}_2-\text{C}_8\text{H}_6\text{N}_2$	□
Alcohol	Serine	Ser	$-\text{CH}_2-\text{OH}$	△
Acid	Aspartic acid	Asp	$-\text{CH}_2-\text{C}(\text{OH})(\text{COOH})$	▲
Amide	Asparagine	Asn	$-\text{CH}_2-\text{C}(\text{NH}_2)(\text{CONH}_2)$	■
Base	Histidine	His	$-\text{CH}_2-\text{C}_3\text{H}_3\text{N}_2$	◇

which appear on the spectrum during the photoirradiation period, when the lifetime of the reaction intermediates is long enough and the quantity is sufficient for detection. Therefore, for the elucidation of the reaction mechanism, it would be an advantageous technique. Recently, we investigated the photodecomposition procedure of L-alanine for various kinds of  $\text{TiO}_2$  photocatalysts with different properties (particle size, surface area, and crystal structure) by  $^1\text{H}$  NMR spectroscopy.<sup>21</sup> On the basis of the identification of several intermediates, we indicated that the photocatalytic procedures for L-alanine are different for individual photocatalysts. Thus, the properties of  $\text{TiO}_2$  evidently influence the photocatalysis of amino acids. In the present study, we employed a popular form of  $\text{TiO}_2$  (ST-01; 100% anatase crystal form), investigated the adsorption and decomposition of seven kinds of amino acids with distinctively different side chain characteristics by  $^1\text{H}$  NMR spectroscopy along with the measurements of the zeta potential of  $\text{TiO}_2$  (ST-01) in amino acid solutions, and compared the photoreactivity and adsorbability of the amino acids.

### Experimental Section

The photocatalyst powders used were  $\text{TiO}_2$  (ST-01) and calcined ST-01 at 973 K. ST-01 was a generous gift from Ishihara Techno and was used as received. The crystal form is 100% anatase with a BET surface area of  $320 \text{ m}^2 \text{ g}^{-1}$  and a particle size of 9 nm.<sup>22</sup> The calcined powders were prepared by calcination in an electric furnace for 3 h at 973 K under air and stored in a capped glass vial under ambient conditions as noncalcined samples. After calcination, the BET surface area and particle size became  $21 \text{ m}^2 \text{ g}^{-1}$  and 53 nm, respectively. The crystal phase was 100% anatase even after calcination at 973 K, which is consistent with our previous measurements.<sup>22,26</sup>

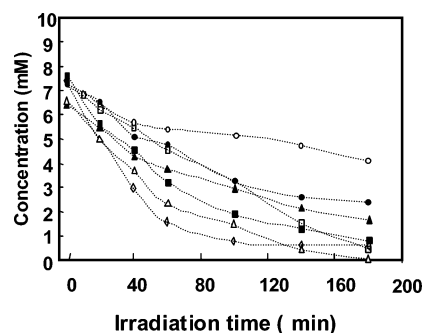


**Figure 1.** Change in the amino acid concentrations in a  $\text{TiO}_2$  photocatalyst suspension, showing the decrease from 10 mM by adsorption, and the decay with irradiation time by photocatalytic decomposition for seven amino acids: Phe (○), Ala (●), Asp (▲), Trp (□), Asn (■), His (◇), and Ser (△).

The seven amino acids examined in the present study (Table 1) were supplied by Wako Pure Chemical. They were selected by taking into account the characteristics of the functional groups of the side chain. Photocatalytic reactions were carried out in an NMR tube of 5 mm diameter.  $\text{TiO}_2$  powder (4.9 mg) was dispersed in a 10 mM ( $M = \text{mol dm}^{-3}$ ) solution of amino acids in 0.5 mL of  $\text{D}_2\text{O}$  (99.9% Isotec, Inc.). The final pH was in the range of 6–7.5 except that of Asp (pH 3.7). The pH was not adjusted to avoid the effect of the counterions on the photocatalytic reactions.  $^1\text{H}$  NMR spectra of amino acids were measured with a JEOL EX-400 spectrometer at 400 MHz. The amount of amino acid adsorbed on the  $\text{TiO}_2$  surface was estimated from the difference in the NMR signal intensities measured before and 12 h after the addition of  $\text{TiO}_2$ . The sample was photoirradiated with three 4-W black light bulbs surrounding the NMR sample tube under aerobic conditions. The sample tube was rotated during irradiation to maintain the powder suspension. The incident light with the wavelength range of 320–380 nm was about  $1 \text{ mW cm}^{-2}$  for each light bulb. To measure the concentration change of the reactant, the NMR spectra were recorded at intervals over the total irradiation time of 3 h. The concentration of the amino acid in the solution was estimated by taking the peak area relative to that of the external standard of DSS (2,2-dimethyl-2-silapentane-5-sulfonate sodium salt) in a glass capillary.

For zeta potential measurements, a 10 mM amino acid solution containing 1 mM  $\text{KNO}_3$  was prepared first, and then a very small amount of  $\text{TiO}_2$  powder was added so as to be observed as an individual  $\text{TiO}_2$  particle in the microscope field with 1 mm depth. The pH was adjusted with KOH and  $\text{HNO}_3$ . The zeta potential was measured with a zeta potential analyzer (Zeecom, ZC-1500), which monitors the electrophoretic speed of particles and calculates the average zeta potential for each solution assuming a spherical shape for the  $\text{TiO}_2$  particles. The water was purified with a Milli-Q water ion-exchange system (Millipore Co.) to give a resistivity of  $1.8 \times 10^7 \Omega \text{ cm}^{-1}$ .

### Results and Discussion

The changes in the concentrations of seven amino acids were plotted against irradiation time in Figure 1. The initial concentration of an amino acid was 10 mM. Photoirradiation was started 12 h after the addition of  $\text{TiO}_2$  to the solution. The decrease in amino acid concentration from 10 mM at irradiation time 0 min corresponds to the amount of adsorbed molecules as described above. The photocatalytic decomposition rates were calculated from the initial slope in Figure 1 for individual amino acids and are summarized in Figure 2, together with the amounts of adsorption.

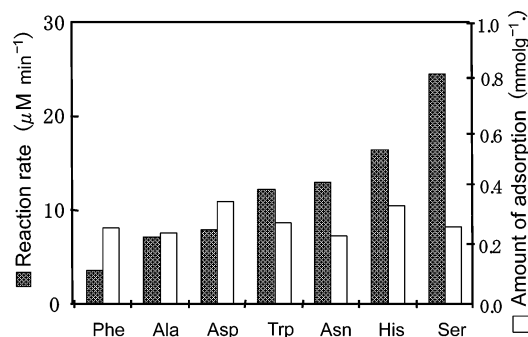


**Figure 2.** Photocatalytic degradation rates (■) of amino acids calculated from the initial decay of the reactant and the amount of adsorption (□) estimated from the decrease in solution concentration.

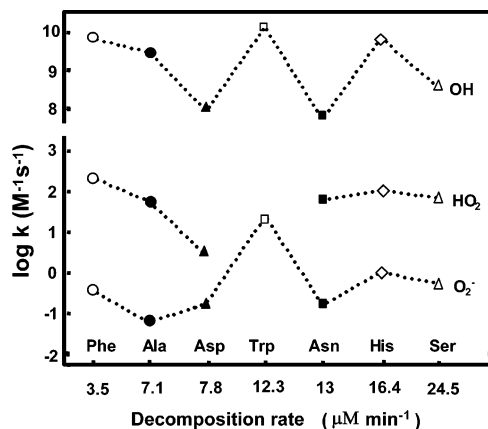


**Figure 3.** Correlation between the photocatalytic decomposition rates and the bimolecular rate constants  $k^{23}$  of the amino acids with active oxygen radicals: OH•, HO₂•, and O₂•⁻.

A significant difference in the amount of adsorption was not observed among the seven amino acids, although the amounts of adsorption for His and Asp were slightly higher than the others. On the other hand, all of the seven amino acids were sensitive to photocatalytic oxidation and some of the amino acids were more vulnerable than the others. The decomposition rates ranged from 3.5 to 24.5  $\mu\text{M min}^{-1}$  and increased in the order of Phe < Ala < Asp < Trp < Asn < His < Ser. It is noted that the amino acids which contain -OH (Ser), -NH (Trp, His), or -NH<sub>2</sub> (Asn) in their side chain degraded faster than the others. For proteins (serum albumin, ovalbumin, and gamma globulin), it was reported that the constituent amino acids were decomposed in the order of Asp < Ser and Phe < His.<sup>14</sup> The mineralization rates of the amino acids, as evidenced by the formation of carbon dioxide, were reported to vary in the order of Phe < Ala < Ser.<sup>19</sup>

In the photocatalytic decomposition of amino acids, photo-induced active species such as trapped holes, OH radicals, peroxide radicals (HO<sub>2</sub>•) and superoxide radical anions (O<sub>2</sub>•⁻) are suspected to be involved and the reactivity with these species is an important factor for the decomposition rates. Therefore, the photodecomposition rates of amino acids obtained in the present study were compared with the bimolecular rate constants reported for the amino acids with those active species.<sup>23</sup> Among these active species, a superoxide radical anion (O<sub>2</sub>•⁻) appears to be less reactive with the amino acids examined except for Trp, as shown in Figure 3. The aromatic amino acids (Phe, Trp, and His) are reactive with both the OH radicals (surface holes) and peroxide radicals (HO<sub>2</sub>•). Asp is reactive with none of the active species, which might explain the relatively low photodecomposition rate of Asp. Ser and Asn show high reactivity

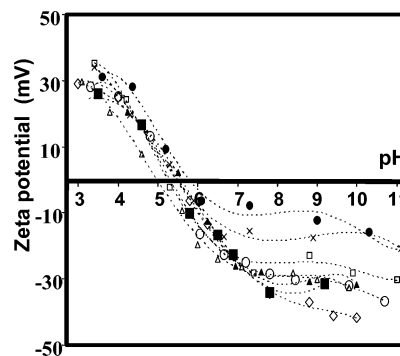


**Figure 4.** Zeta potentials of TiO<sub>2</sub> in an aqueous suspension (×) and in solutions containing various amino acids: Phe (○), Ala (●), Asp (▲), Trp (□), Asn (■), His (◇), and Ser (△).

with the peroxide radicals (HO<sub>2</sub>•) but not with the OH radicals. Thus, although reactivity with active species is an important factor, by taking into account the fact that the adsorbed amount is almost the same for all of the amino acids, the difference in the decomposition rates could not be attributed only to the difference in the bimolecular rate constant. For example, Phe shows high reactivity with both OH radicals and peroxide radicals (HO<sub>2</sub>•), but the observed photodecomposition rate was very low. This is partly because the photodecomposition of the amino acids does not follow a simple reaction between these free radicals and amino acids. Besides, there must be other important factors that affect the decomposition of amino acids. The surface states of TiO<sub>2</sub> photocatalysts and their interactions with each of the amino acids must play an important role.

To obtain information about the adsorbed states of amino acids in aqueous suspension, the zeta potential was measured by changing the pH. As shown in Figure 4, upon adsorption of amino acids, the zeta potential shifted to the negative direction with respect to the control anatase suspension over the entire tested pH range for Ser, Trp, Phe, His, and Asn and to the positive direction for Ala, and it was almost unchanged for Asp. The value of the isoelectric point (IEP), which is defined by the pH having zero potential, ranged from 5.0 to 5.8, depending on the properties of the amino acids. The IEP value without the amino acids was 5.5. Taking into account that the side chain groups of Ala, Ser, Trp, Phe, His, and Asn carry no charge, the shift direction of the zeta potential on the adsorption is expected to be the same. However, as shown in Figure 4, this was not the case, suggesting that the adsorption part is different for Ala and the other four amino acids. On the surface of TiO<sub>2</sub>, there are two kinds of hydroxyl groups: bridged OH and terminal OH. The bridged OH is acidic, while the terminal OH is basic.<sup>24–26</sup> The bridged OH is thermally more stable than the terminal OH. On the basis of the effects of thermal treatment on the IEP, it was deduced that the elimination of the terminal OH by the heat treatment to leave the bridged OH on the surface made the TiO<sub>2</sub> surface more acidic.<sup>27</sup> Similarly, the adsorption of the amino acids on the basic terminal sites could enhance the surface acidity of TiO<sub>2</sub> because the contribution of the remaining acidic bridged sites to the surface charge would increase, which would lead the lower shift of the IEP. Thus, the negative shift of the zeta potential observed on the adsorption of five amino acids (Ser, Trp, Phe, His, and Asn) suggests that these amino acids should interact with the terminal OH to make the surface more acidic. On the other hand, the positive shift observed for Ala would indicate an interaction with the bridged OH, which makes the surface more basic. The geometry around the bridged OH on the TiO<sub>2</sub> surface might allow only small



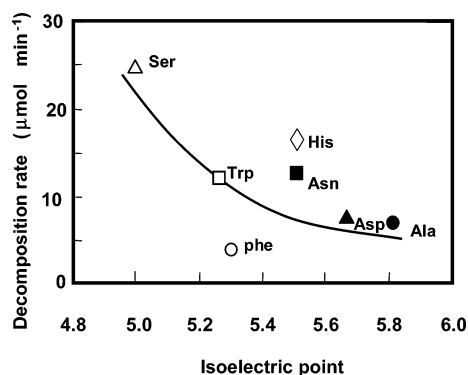


**Figure 5.** Decomposition rates for seven amino acids plotted against the IEP of  $\text{TiO}_2$  powder in the adsorbed state.

amino acids, such as Ala, access to the bridged OH sites. IR measurements indicated that the carboxyl group of Ala bridges the surface titanium.<sup>28</sup>

In Figure 5, the decomposition rate for each amino acid was plotted against the IEP value. The decomposition rate was correlated with the IEP and became higher as the IEP decreased, although some deviations for the aromatic amino acids were observed. This appears to indicate that the stronger adsorption of the amino acids on the basic terminal sites leads to the lower shift in the IEP, resulting in enhanced photocatalytic activity.

$\text{TiO}_2$  is known to show amphiphilic properties. This means that there are both hydrophobic and hydrophilic sites on the solid surface. Hydrophilic sites may include the surface hydroxyl groups. All of the amino acids can interact with the surface by their carboxyl and amino groups and side chains. The adsorption of Gly, Met, Ser, and Cys on partially hydroxylated rutile (100) and (110) surfaces was simulated by first principles molecular dynamics.<sup>29</sup> Although they might not be directly comparable with the anatase  $\text{TiO}_2$  (ST-01) surface used in the present study, more stable configurations are attained by ester condensation of the carboxyl and terminal OH groups and by the formation of a bond between a deprotonated hydroxyl or thiol group of Ser or Cys, respectively, and a surface Ti. On the other hand, Hayden et al. suggested that a hydroxyl group adjacent to the ester bridge is eliminated and a bidentate configuration is obtained in which the carboxyl group of the amino acid replaces two adjacent bridging oxygens.<sup>30</sup> The photodecompositions of two representative compounds, that is, acetic acid and benzoic acid, were investigated by  $^1\text{H}$  NMR spectroscopy for six anatase-abundant  $\text{TiO}_2$  photocatalysts.<sup>27</sup> Both compounds possess carboxyl groups, and for benzoic acid, a methyl group of acetic acid is substituted by an aromatic ring. Because of the difference in the hydrophobicities of the two compounds, they exhibited different adsorbabilities on each photocatalyst and showed different decomposition behaviors. Benzoic acid could be adsorbed through the carboxyl group and/or the aromatic ring on the solid surface. The carboxyl group can interact with the surface hydroxyl groups or adsorbed water molecules to form hydrogen bonds, while the aromatic ring can be adsorbed directly on the hydrophobic sites of the solid surface. Photocatalysis is expected to be more efficient for direct adsorption. Actually, the photocatalytic decomposition of benzoic acid with an aromatic ring was found to be much faster in all of the  $\text{TiO}_2$  aqueous suspensions and more enhanced for the fully dehydroxylated  $\text{TiO}_2$  than that of acetic acid. In the presence of adsorbed water, the binding of a carboxyl group of the molecules with adsorbed water competes with the direct adsorption on the surface, which reduces the amount of the direct adsorption and results in the reduction of photocatalytic efficiency. These results

suggest that the most efficient photocatalytic sites should be the hydrophobic sites on the  $\text{TiO}_2$  surface. This also accounts for the higher photodegradation of benzoic acid compared to that for acetic acid, since the aromatic groups are adsorbed more favorably on the hydrophobic sites of  $\text{TiO}_2$  than the methyl groups.<sup>27</sup>

However, as shown in Figure 5, the typical hydrophobic amino acid Phe showed a very low decomposition rate despite its high reactivity with the active species (Figure 3). Therefore, it is considered that efficient photooxidation through the direct adsorption of a phenyl ring on the hydrophobic sites of  $\text{TiO}_2$  does not take place. Instead, the relatively large lower shift of the IEP observed for Phe suggests that Phe should interact with the terminal OH groups by its carboxyl group or its amino group. The difference in the adsorbability and photocatalytic reactivity between benzoic acid and Phe may be attributed to the molecular structure of Phe possessing an amino group in addition to a carboxyl group, which can interact with the  $\text{TiO}_2$  surface. Hidaka and co-workers reported that, on the photocatalytic oxidation of Phe, the loss of the amine is 10-fold faster than the evolution of carbon dioxide.<sup>18</sup> This fact might support that Phe interacts with the terminal OH by its amino group. Thus, since the typical hydrophobic amino acid Phe was not directly adsorbed on the hydrophobic photocatalytic site, which is the most effective site for benzoic acid, the terminal OH seems to be the favorable photocatalytic site for the amino acids. Although Phe interacts with the terminal OH either by the carboxyl group or the amino group, the decomposition rate is very low. On the other hand, the amino acids possessing  $-\text{OH}$  (Ser),  $-\text{NH}$  (Trp, His), or  $-\text{NH}_2$  (Asn) in their side chain caused an IEP shift to a lower pH upon adsorption and showed high decomposition rates. Therefore, the side chains of these amino acids are considered to interact more favorably with the terminal OH on  $\text{TiO}_2$  than the amino or carboxyl groups, resulting in high decomposition rates. This may be supported by the results reported by Hidaka and co-workers that the rate of loss of the amine for Ser is about 3 times less than that for Phe upon photodecomposition.<sup>19</sup> The OH of Ser seems to interact with the terminal OH very strongly, resulting in the significantly lower shift of the IEP and the high decomposition rate. And, the NH groups of Trp and His are also considered to be capable of interacting strongly with the terminal OH. Actually, the IR measurements indicated the ability of His to bind through the N atom of an imidazole group with the surface OH group on  $\text{TiO}_2$ .<sup>28</sup> Thus, the three potential binding sites of amino acids, that is, an amino group, a carboxyl group, and a side chain, would compete for the interaction with the terminal OH sites, which are considered to be the favorable photocatalytic active sites for amino acids.

To verify the contribution of the surface hydroxyl groups to the photocatalysis of amino acids, we prepared  $\text{TiO}_2$  without hydroxyl groups by heat treatment at 973 K and investigated the adsorption and decomposition on the calcined  $\text{TiO}_2$  photocatalysts by employing two amino acids, Ala and Trp.

It is well-known that thermal treatment can cause a change in crystalline form, particle size, surface area, and oxygen defects, which can significantly influence the electronic and the geometric structures of  $\text{TiO}_2$  and, in turn, alter its chemical reactivity.<sup>31</sup> For ST-01, the crystalline composition did not change before and after calcination at 973 K, while the surface area was drastically reduced and the crystal size was increased, as described in the Experimental Section. For photocatalytic reactions, the importance of substrate preadsorption and, thus, surface area has been acknowledged. However, a clear relationship between surface area and photocatalytic activity has not

been demonstrated for photocatalysis by TiO<sub>2</sub>.<sup>27,32</sup> Krýsa et al. prepared two types of TiO<sub>2</sub> photocatalysts which exhibit a rather large surface area (300 m<sup>2</sup> g<sup>-1</sup>) and small particle size (3–4 nm) and consist of round agglomerates (1–2 μm). Although the surface area significantly decreased after thermal treatment at 873 K, the degradation rate of oxalic acid and 4-chlorophenol did not. Therefore, they suggested that the surface area is not the most important parameter.<sup>33</sup> Furthermore, we found that for the case of ST-01, after calcination at 973 K, the photocatalytic oxidation of benzoic acids and acetic acids was notably enhanced despite the decrease in the surface area.<sup>27</sup> In general, the increase in a catalyst crystal size is detrimental to catalytic activity since it results in the reduction of the reactant/catalyst contact area. However, Yu et al. concluded that the enhancement in photocatalytic activity after thermal treatment cannot be attributed to the growth of the crystal size since no increase in crystal size was found in the samples after thermal treatment at 473 and 573 K but the two samples exhibited an enhancement in photoactivity.<sup>34</sup> Therefore, there must be other more important factors that affect photocatalytic activity. Previously, we investigated the effects of thermal treatment on photocatalytic activity by <sup>1</sup>H NMR spectroscopy for various TiO<sub>2</sub> photocatalysts with different properties and demonstrated that the surface hydroxyl groups play an important role in photocatalytic activity.<sup>27</sup>

TiO<sub>2</sub> contains both terminal and bridged OH groups on the surface before calcination. For TiO<sub>2</sub> calcined at 623 K, most of the terminal OH groups were eliminated upon heat treatment, and at 973 K, both the terminal and bridged OH groups are considered to be eliminated, although a small amount of the bridged OH groups are reported to still be present,<sup>35</sup> which makes the surface highly hydrophobic.<sup>27</sup>

Recently, we investigated the effects of thermal treatment on the rehydration process by <sup>1</sup>H NMR spectroscopy for six anatase-abundant TiO<sub>2</sub> photocatalysts with different properties.<sup>27</sup> After calcination at 623 K, under ambient conditions, the water molecules in the air were rapidly readsorbed on the TiO<sub>2</sub> surface, forming the adsorbed water layers. On the other hand, after calcination at 973 K, the physisorbed water layers recovered relatively fast for P25, F4, and AMT-600 (shorter than 24 h) with no significant enhancement of the photocatalytic decomposition. (Acetic acid and benzoic acid were employed for photodecomposition in an aqueous suspension.) On the other hand, for ST-01, UV-100, and AMT-100, the recovery was very slow (longer than one week) and only partially reversible and the photocatalytic decomposition was considerably enhanced despite the decrease in the surface area.<sup>27</sup> For ST-01, the water layer barely recovered at more than one month after the thermal treatment at 973 K. Thus, it was revealed that ST-01 calcined at 973 K could keep the hydrophobic surface for a fairly long time, even in aqueous solution.<sup>27</sup> Therefore, it is expected that, with ST-01 calcined at 973 K, the effect of the surface OH on the adsorption and photocatalytic activity of amino acids can be derived more evidently.

The changes in the concentrations of Ala and Trp in an aqueous suspension of TiO<sub>2</sub> calcined at 973 K were plotted against irradiation time together with those in a noncalcined TiO<sub>2</sub> suspension, as shown in Figure 6. The initial concentration of all of the amino acids was 10 mM. The decrease in concentration from 10 mM at irradiation time 0 min corresponds to the amount of adsorbed molecules, as described above. It is clear that, for TiO<sub>2</sub> calcined at 973 K, the amount of adsorbed amino acids and the decomposition rates were substantially decreased both for Ala and Trp as compared to those for

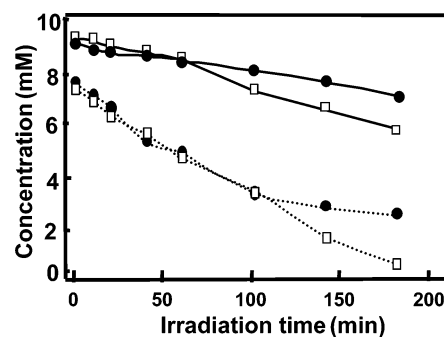


**Figure 6.** Change in the concentrations of Ala (●) and Trp (□) upon adsorption and photoirradiation with TiO<sub>2</sub> powders: noncalcined (···) and calcined at 973 K (—). The initial amino acid concentrations were 10 mM.

noncalcined TiO<sub>2</sub>. Thus, the elimination of the surface hydroxyl groups evidently reduced the adsorption and photodecomposition of the amino acids, indicating that the surface hydroxyl groups actually do play very important roles in the photocatalysis of amino acids on TiO<sub>2</sub>. The photocatalytic oxidation of hydrophobic molecules, such as benzoic acid, was notably enhanced on a TiO<sub>2</sub> (ST-01) surface calcined at 973 K in an aqueous suspension system. Because the aromatic ring is favorably adsorbed directly on the hydrophobic surface, it is effectively photodecomposed.<sup>27</sup> However, this seems to not be the case for aromatic amino acids. The present results suggest that, unlike benzoic acids, Trp should not be photooxidized effectively by adsorption on the hydrophobic sites of the TiO<sub>2</sub> surface. Unlike benzoic acid, aromatic amino acids possess an amino group in addition to a carboxyl group and an aromatic side chain. In the solution pH range for the NMR measurements, it exists in a zwitterionic form of  $-\text{COO}^-$  and  $-\text{NH}_3^+$ , whose interaction/binding with the water molecules around the TiO<sub>2</sub> surface would compete with the interaction with the hydrophobic sites on the TiO<sub>2</sub> surface. The zwitterionic form of the amino acids might be highly stabilized by the interaction with the surrounding water molecules to prevent the amino acids from directly accessing the hydrophobic sites of TiO<sub>2</sub>. However, in the presence of the surface hydroxyl groups, the functional groups of the amino acids could directly interact with the TiO<sub>2</sub> surface.

As shown in Figure 7, for TiO<sub>2</sub> calcined at 973 K, the zeta potential in the absence of amino acids shifted to the negative direction, and the IEP decreased from 5.5 to 4.2, indicating that the TiO<sub>2</sub> surface became more acidic after calcination at 973 K. This negative shift of the IEP could be attributed to the removal of the terminal OH groups by the calcination of TiO<sub>2</sub>, which has basic properties. Bridged OH is known to be thermally more stable than terminal OH and is reported to be present in small quantities, even after evacuation at 973 K.<sup>35</sup> The zeta potentials for Ala and Trp showed almost the same profile as those without amino acids. Thus, after the elimination of both terminal and bridged OH groups, the zeta potential remains unchanged upon addition of the amino acids, indicating that the interaction that affects the surface charge by the adsorption of amino acids was suppressed.

Thus, it is reasonably deduced that, as stated above, Trp interacts with the terminal OH group on the noncalcined TiO<sub>2</sub> by the side chain to cause the zeta potential to shift to the negative direction and shows a high decomposition rate. On the other hand, Ala interacts with the bridged OH group most probably by the carboxyl group to cause the zeta potential to shift to the positive direction and shows a relatively low decomposition rate. The plausible interaction modes of Ala and Trp on the noncalcined TiO<sub>2</sub> surface are illustrated in Figure 8.

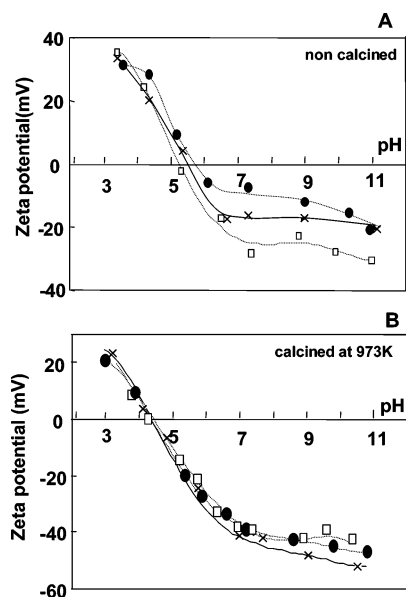


**Figure 7.** Zeta potentials of  $\text{TiO}_2$  powders (A, noncalcined; B, calcined at 973 K) measured in pure aqueous suspensions (x) and in Ala (●) and Trp (□) solutions at various pH values.

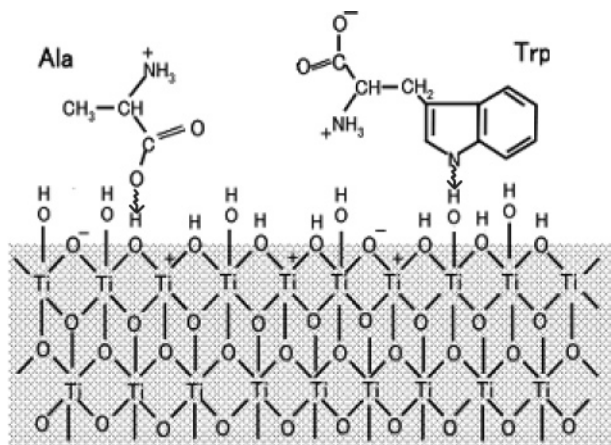


**Figure 8.** Plausible structure representing the interactions of Ala and Trp with the noncalcined  $\text{TiO}_2$  surface. Adsorbed water molecules are not shown for clarity.

Ala binds to the  $\text{TiO}_2$  surface through the carboxyl group, while Trp binds through the nitrogen atom of the heterocyclic ring.

Although the binding of the carboxyl groups by the amino acids on the  $\text{TiO}_2$  surface is generally acknowledged,<sup>28–30</sup> the present study suggests that the interaction of the three functional groups of amino acids (carboxyl and amino groups and side chain) with the surface OH groups on  $\text{TiO}_2$  should be a key factor for understanding the adsorption and decomposition of proteins/peptides on  $\text{TiO}_2$  photocatalysts. However, taking into account that the adsorption amount of all of the amino acids on noncalcined  $\text{TiO}_2$  powders was almost the same but that the induced IEP shift was different, there must be other adsorption sites on  $\text{TiO}_2$  which are less active in terms of photocatalysis.

## Conclusions

By measuring the zeta potential of  $\text{TiO}_2$  aqueous suspension systems for seven kinds of amino acids, it was found that the adsorption of the amino acids on the  $\text{TiO}_2$  surface caused the change in the acidity of the  $\text{TiO}_2$  surface, which is attributed to the interaction of the amino acids with the basic terminal OH or acidic bridged OH groups on the solid surface. The

photodecomposition rates of the amino acids on the  $\text{TiO}_2$  surface obtained by  $^1\text{H}$  NMR increased in the order of Phe < Ala < Asp < Trp < Asn < His < Ser and correlated with the changes in the IEP on adsorption. Since the IEP shifted to a lower pH with increasing decomposition rates for Phe, Trp, Asn, His, and Ser, the effective adsorption and photocatalytic sites for these amino acids are considered to be the basic terminal OH groups. Phe, which shows a low photodecomposition rate, is considered to be adsorbed by the amino group; however, the amino acids containing  $-\text{OH}$  (Ser),  $-\text{NH}$  (Trp, His), or  $-\text{NH}_2$  (Asn) in their side chain appeared to be adsorbed more favorably by the side chain to be more vulnerable to photocatalytic oxidation and showed high decomposition rates. On the other hand, Ala interacts with the acidic bridged OH groups on  $\text{TiO}_2$  to cause an IEP shift to a higher pH. The correlation of the surface hydroxyl groups with the photocatalysis of amino acids was verified by the use of calcined  $\text{TiO}_2$  without surface hydroxyl groups. With the  $\text{TiO}_2$  calcined at 973 K, a significant reduction in the decomposition rates and adsorption amounts on the surface was observed and the zeta potentials of the  $\text{TiO}_2$  aqueous suspension on addition of Trp or Ala were the same as those without amino acids. Thus, from the present study, it was evidently deduced that the surface hydroxyl groups play a key role in the adsorption and photodecomposition of amino acids.

**Acknowledgment.** This work was supported in part by a Grant-in-Aid on Priority Areas (417), a 21st COE Program (for T.H.T.) from the Ministry of Education, Culture, Science, and Technology (MEXT), and also Core Research for Evolution Science and Technology (CREST) under the auspices of the Japan Science and Technology Agency (JST).

## References and Notes

- (1) *Photocatalytic Purification and Treatment of Water and Air*; Ollis, O., El-Akabi, H., Eds.; Elsevier: New York, 1993.
- (2) Fujishima, A.; Hashimoto, K.; Watanabe, T.  *$\text{TiO}_2$  Photocatalysis: Fundamentals and Application*; BKC Publishing: Tokyo, 1999.
- (3) *Photocatalysis—Science and Technology*; Kaneko, M., Ohkura, I., Eds.; Kodansha-Springer: Tokyo, 2002.
- (4) Hoffmann, M. R.; Martin, S. T.; Choi, W.; Bahnemann, D. W. *Chem. Rev.* **1995**, *95*, 69.
- (5) Mills, A.; Hunte, S. L. *J. Photochem. Photobiol., A* **1997**, *108*, 1.
- (6) Fujishima, A.; Rao, T. N.; Tryk, D. A. *J. Photochem. Photobiol., C* **2000**, *1*, 1.
- (7) Peterson, M. W.; Turner, J. A.; Nozik, A. J. *J. Phys. Chem.* **1991**, *95*, 221.
- (8) Cooper, G.; Nozik, A. *Novel and Simple Approach to Elimination of Dilute Toxic Wastes Based on Photoelectrical Systems*; EPA/600/2-89/007 (NTIS PB89161855); U.S. Environmental Protection Agency: Washington, DC, 1989.
- (9) Sunada, K.; Watanabe, T.; Hashimoto, K. *J. Photochem. Photobiol., A* **2003**, *156*, 227.
- (10) Amezcaga-Madrid, P.; Silveyra-Morales, R.; Cordoba-Fierro, L.; Nevarez-Moorillon, G. V.; Miki-Yoshida, M.; Orrantia-Borunda, E.; Solis, F. J. *J. Photochem. Photobiol., B* **2003**, *70*, 45.
- (11) Lu, Z.-X.; Zhou, L.; Zhang, Z.-L.; Shi, W.-L.; Xie, Z.-X.; Xie, H.-Y.; Pang, D.-H.; Shen, P. *Langmuir* **2003**, *19*, 8765.
- (12) Kubota, Y.; Shuin, T.; Kawasaki, C.; Hosaka, M.; Kitamura, H.; Cai, R.; Sakai, H.; Hashimoto, K.; Fujishima, A. *Br. J. Cancer* **1994**, *70*, 1107.
- (13) Saito, T.; Iwase, T.; Horie, J.; Morioka, T. *J. Photochem. Photobiol., B* **1992**, *14*, 369.
- (14) Muszkat, L.; Feigelson, L.; Bir, L.; Muszkat, K. A. *J. Photochem. Photobiol., B* **2001**, *60*, 32.
- (15) Muszkat, L.; Feigelson, L.; Bir, L.; Muszkat, K. A. *Pest Manage. Sci.* **2002**, *58*, 1143.
- (16) Hayashi, T.; Sano, K.; Shiba, K.; Kumashiro, Y.; Iwahori, K.; Yamashita, I.; Hara, M. *Nano Lett.* **2006**, *6*, 515.
- (17) Sano, K.; Shiba, K. *J. Am. Chem. Soc.* **2003**, *125*, 14234.
- (18) Hidaka, H.; Horikoshi, S.; Ajisaka, K.; Zhao, J.; Serpone, N. *J. Photochem. Photobiol., A* **1997**, *108*, 197.
- (19) Horikoshi, S.; Serpone, N.; Zhao, J.; Hidaka, H. *J. Photochem. Photobiol., A* **1998**, *118*, 123.
- (20) Martra, G.; Horikoshi, S.; Anpo, M.; Coluccia, S.; Hidaka, H. *Res. Chem. Intermed.* **2002**, *28*, 359.



- (21) Matsushita, M.; Tran, T. H.; Nosaka, A. Y.; Nosaka, Y. *Cat. Today*, in press.
- (22) Nosaka, Y.; Nakamura, M.; Hirakawa, T. *Phys. Chem. Chem. Phys.* **2002**, *4*, 1088.
- (23) Buxton, G. V.; Greenstock, C. L.; Helman, W. P.; Ross, A. B. *J. Phys. Chem. Ref. Data* **1988**, *17*, 513.
- (24) Parfitt, G. D. *Prog. Surf. Membr. Sci.* **1976**, *11*, 181.
- (25) Boehm, H. P. *Discuss. Faraday Soc.* **1971**, *52*, 264.
- (26) Nosaka, A. Y.; Nosaka, Y. *Bull. Chem. Soc. Jpn.* **2005**, *78*, 1595.
- (27) Nosaka, A. Y.; Nishino, J.; Fujiwara, T.; Yagi, H.; Akutsu, H.; Nosaka, Y. *J. Phys. Chem. B* **2006**, *110*, 8380.
- (28) Ruvarac-Bugaric, I. A.; Saponjic, Z. V.; Zec, S.; Rajh, T.; Nedeljkovic, J. M. *Chem. Phys. Lett.* **2005**, *407*, 110.
- (29) Langel, W.; Menken, L. *Surf. Sci.* **2003**, *538*, 1.
- (30) Hayden, B. E.; King, A.; Newton, M. A. *J. Phys. Chem. B* **1999**, *103*, 203.
- (31) Primet, M.; Pichat, P.; Mathieu, M. V. *J. Phys. Chem.* **1971**, *75*, 1216.
- (32) Porter, J. F.; Li, YU-G.; Chan, C. K. *J. Mater. Sci.* **1999**, *34*, 1523.
- (33) Krýsa, J.; Keppert, M.; Jirkovský, J.; Štengl, V.; Šubrt, J. *Mater. Chem. Phys.* **2004**, *86*, 333.
- (34) Yu, J. C.; Lin, J.; Lo, D.; Lam, S. K. *Langmuir* **2000**, *16*, 7304.
- (35) Hadjiivanov, K. I.; Klissurski, D. G. *Chem. Soc. Rev.* **1996**, *25*, 61 and references therein.